THE UNIVERSITY OF RHODE ISLAND

University of Rhode Island
DigitalCommons@URI

Biomedical and Pharmaceutical Sciences Faculty Publications

Biomedical and Pharmaceutical Sciences

2024

Unbound Fractions of PFAS in Human and Rodent Tissues: Rat Liver a Suitable Proxy for Evaluating Emerging PFAS?

Sangwoo Ryu

Woodrow Burchett

Sam Zhang

Xuelian Jia

Seyed Mohamad Sadegh Modaresi

See next page for additional authors

Follow this and additional works at: https://digitalcommons.uri.edu/bps_facpubs

Unbound Fractions of PFAS in Human and Rodent Tissues: Rat Liver a Suitable Proxy for Evaluating Emerging PFAS?

Authors

Sangwoo Ryu, Woodrow Burchett, Sam Zhang, Xuelian Jia, Seyed Mohamad Sadegh Modaresi, Juliana Agudelo Areiza, David Rodrigues, Hao Zhu, Elsie M. Sunderland, Fabian Christoph Fischer, and Angela Slitt

The University of Rhode Island Faculty have made this article openly available. Please let us know how Open Access to this research benefits you.

This is a pre-publication author manuscript of the final, published article.

Terms of Use

This article is made available under the terms and conditions applicable towards Open Access Policy Articles, as set forth in our Terms of Use.

Unbound fractions of PFAS in Human and Rodent Tissues: Rat liver a suitable proxy for evaluating emerging PFAS?

Sangwoo Ryu[1,2], Woodrow Burchett[2], Sam Zhang[2], Xuelian Jia[4,5], Seyed Mohamad Sadegh Modaresi[1], Juliana Agudelo[1], David Rodrigues[2], Hao Zhu[4,5], Elsie M. Sunderland[3], Fabian Christoph Fischer[1,3,], Angela L. Slitt[1,*]*

[1] Department of Biomedical and Pharmaceutical Sciences, University of Rhode Island, Kingston, RI United States.

[2] Pharmacokinetics, Dynamics and Metabolism, Pfizer Worldwide Research & Development, Pfizer Inc., Groton, CT 06340 United States.

[3] Harvard John A. Paulson School of Engineering and Applied Sciences, Harvard University, Cambridge, Massachusetts 02138, United States.

[4] Department of Chemistry and Biochemistry, Rowan University, Glassboro, NJ, 08028, United States.

[5] Center for Biomedical Informatics and Genomics, Tulane University, New Orleans, Louisiana, 70112, United States.

*Address correspondence to: angela_slitt@uri.edu, fabian.fischer@uri.edu

Abstract

Adverse health effects associated with exposures to per- and polyfluoroalkyl substances (PFAS) are a concern for public health and are driven by their elimination half-lives and accumulation in specific tissues. However, data on PFAS binding in human tissues are limited. Accumulation of PFAS in human tissues has been linked to interactions with specific proteins and lipids in target organs. Additional data on PFAS binding and unbound fractions ($f_{unbound}$) in whole human tissues are urgently needed. Here we address this gap by using rapid equilibrium dialysis to measure the binding and $f_{unbound}$ of 16 PFAS with 3 to 13 perfluorinated carbon atoms (η_{pfc} = 3-13) and several functional head-groups in human liver, lung, kidney, heart, and brain tissue. We compare results to mouse (C57BL/6 and CD-1) and rat tissues. Results show that $f_{unbound}$ decreases with increasing fluorinated carbon chain length and hydrophobicity. Among human tissues, PFAS binding was generally greatest in brain>liver≈kidneys≈heart>lungs. A correlation analysis among human and rodent tissues identified rat liver as suitable surrogate for predicting $f_{unbound}$ for PFAS in human tissues (R^2 ≥0.98). The $f_{unbound}$ data resulting from this work and the rat liver prediction method offer input parameters and tools for toxicokinetic models for legacy and emerging PFAS.

Synopsis: Similar PFAS binding in human and rodent tissues suggests rat liver is a useful model tissue for predicting PFAS accumulation and tissue distribution in humans.

Keywords: PFAS, unbound fractions, tissue binding, species correlation, equilibrium dialysis

TOC Art

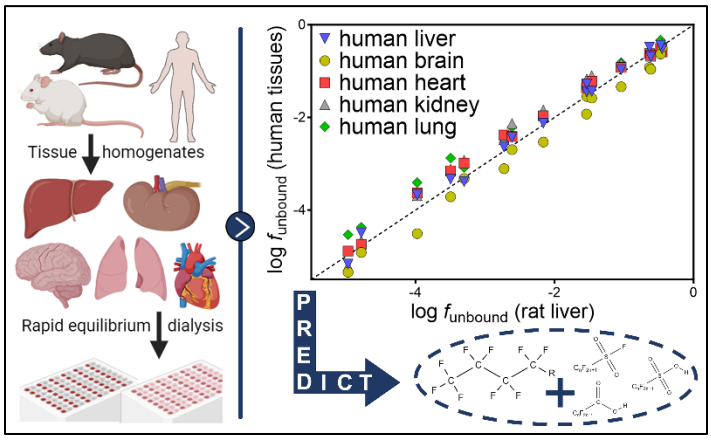
Tissue
homogenates
Rapid equilibrium
dialysis
human liver
human brain
human heart
human kidney
human lung
log $f_{unbound}$ (human tissues)
log $f_{unbound}$ (rat liver)
0
-2
-4
PREDICT

1. Introduction

Per- and polyfluorinated alkyl substances (PFAS) are a diverse class of anthropogenic chemicals with a wide range of commercial and industrial applications.[1] Their extensive use has resulted in detectable concentrations in drinking water, ambient air, animals, and in virtually all humans.[1-13] PFAS exposures are associated with adverse health outcomes, such as thyroid hormone disruption, decreased response to vaccination,[14] dyslipidemia,[15] and hepatotoxicity.[16] Slow elimination and strong tissue accumulation of PFAS are typically associated with increased toxicity.[17] While hundreds of PFAS have been detected in the environment, tissue-specific accumulation has been tested only for a handful of PFAS.[18] Accumulation and slow elimination of PFAS in humans have been associated with binding to isolated biomolecules;[19-21] however, they have not yet been linked to PFAS binding to whole tissues. Data and predictive tools for characterizing PFAS binding in whole human tissues are needed and are the focus of this work.

PFAS with long fluorinated carbon chains ($\eta_{pfc} \geq 7$), such as perfluorooctanoic acid (PFOA, $\eta_{pfc} = 7$) and perfluorooctane sulfonic acid (PFOS, $\eta_{pfc} = 8$), show strong accumulation in humans and have elimination half-lives that range between 3-6 years.[22-24] In contrast, short-chain PFAS like perfluorobutanoic acid (PFBS, $\eta_{pfc} = 3$) are eliminated by humans in weeks.[25] After absorption in the gastrointestinal tract, PFAS pass through liver and enter the circulatory system.[21,26-28] For PFAS with $\eta_{pfc} \geq 7$, binding to proteins and phospholipids are thought to determine elimination half-lives.[29-31] For PFAS with $\eta_{pfc} < 6$, membrane transporters, enterohepatic recirculation, and renal tubular reabsorption may play a more important role in tissue distribution.[31,32] Binding of PFAS to tissues is driven by their physicochemical properties (e.g., η_{pfc}, hydrophobicity, p*K*a), the macromolecular composition of the tissue (e.g., structural proteins, phospholipids), and abundantly expressed functional proteins (e.g., fatty acid binding proteins and albumin).[33,34] An increasing number of structurally diverse PFAS means there is a need to systematically characterize PFAS binding to human tissues and identify the physicochemical properties that

drive tissue accumulation. However, PFAS binding to human tissues beyond plasma have not yet been measured.

The unbound fraction of chemicals ($f_{unbound}$) in tissues is typically the amount that is available for inter-tissue transport and interacts with molecular targets that elicit toxic effects.[35] $f_{unbound}$ is inversely correlated to the tissue binding affinity, which can be quantified by the tissue-water partition coefficient ($K_{tissue/w}$).[31] PFAS that are bound to tissue components (e.g., proteins, phospholipids) are considered unavailable for renal and hepatic clearance until being desorbed as unbound PFAS are eliminated,[36-38] thereby prolonging elimination half-lives. At steady-state, unbound concentrations ($C_{unbound}$) are expected to be similar among tissues, assuming negligible influence of membrane transporter-mediated flux.[39] $f_{unbound}$ and $K_{tissue/w}$ can be used to predict tissue-specific accumulation and elimination half-lives. Comprehensive studies on experimental $f_{unbound}$ and $K_{tissue/w}$ in whole human tissues are urgently needed to assess PFAS accumulation and tissue distribution in humans.

Previous studies measured PFAS binding to isolated macromolecules, such as proteins (bovine serum albumin [BSA][40,41], human serum albumin [HSA][42], fatty-acid binding protein [FABP][43]) and phospholipids.[44] Partition coefficients derived from such studies have been used to parameterize physiologically-based toxicokinetic (PBTK) models and simulate $f_{unbound}$ and the tissue distribution of PFAS.[19,20,29,31] Machine-learning and molecular dynamics simulations are *in silico* substitutes to experimental derivation of $f_{unbound}$ and tissue binding.[45] While these simulations provide mechanistic insights into the interaction of PFAS with single biomolecules,[38] they have rarely been evaluated against experimental $f_{unbound}$ in whole tissues. Rodent tissues have been used to generate data on $f_{unbound}$ for diverse pharmaceuticals that were useful for predicting $f_{unbound}$ in human tissues.[46-49] Extending tissue partitioning measurements for PFAS in rodents to humans might similarly be useful.

The main objective of this work was to evaluate the suitability of $f_{unbound}$ and $K_{tissue/w}$ measured in rodent model tissues for predicting PFAS binding in human tissues. Furthermore,

this is the first study to report unbound fractions in various human tissues. This study leverages a well-established framework for pharmaceuticals and a high-throughput equilibrium dialysis method[50-52] to measure $f_{unbound}$ and $K_{tissue/w}$ of 16 PFAS with η_{pfc} 3–13 and different functional head groups (carboxylic acids, sulfonic acids, and sulfonamides) in brain, heart, kidney, liver, and lung tissues of humans and rodents (mouse, rat). These tissues were selected because they have been shown to accumulate PFAS in humans.[19,21] Inter-species and -tissue correlation analyses were used to evaluate how well various rodent tissues predicted $f_{unbound}$ in human tissues. Regression modeling was applied to assess the relationship between physicochemical properties of PFAS and their $f_{unbound}$ in various tissues. Using our data, we discuss potential mechanisms driving PFAS toxicokinetics in humans and the suitability of rodent surrogate tissues as a fast and straightforward tool for predicting human PFAS tissue distribution.

2. Materials and Methods

2.1 Chemicals and Reagents.

The study PFAS included 11 perfluoroalkyl carboxylates, 3 perfluoroalkyl sulfonates, 1 perfluoroalkyl sulfonamide, and 1 fluorotelomer sulfonate. Physicochemical properties of PFAS ranged from η_{pfc} from 3 to 13, molecular weight (M_w) from 214.04 to 714.11 g/mol, p*K*a from -0.21 to 6.25, [53] and octanol-water distribution coefficients (log*D*, pH: 7.0) from 2.23 to 10.11 (Tables S1 and S2). Standards for perfluorobutanoic acid (PFBA), perfluoropentanoic acid (PFPA), perfluorohexanoic acid (PFHxA), perfluoroheptanoic acid (PFHpA), perfluorooctanoic acid (PFOA), perfluorononanoic acid (PFNA), perfluorodecanoic acid (PFDA), perfluoroundecanoic acid (PFUDA), perfluorododecanoic acid (PFDoDA), perfluorotridecanoic acid (PFTriDA), perfluorotetradecanoic acid (PFTeDA), perfluorohexane sulfonic acid (PFHxS), perfluorooctanesulfonamide (PFOSA), and 6:2 fluorotelomer sulfonate (6:2 FtS) were purchased from AccuStandard. Standards for perfluorobutane sulfonic acid (PFBS) and perfluorooctane sulfonic acid (PFOS) were purchased from Sigma-Aldrich. Brain, heart, kidney, liver, and lung from commonly used rat and mouse strains (Wistar Han rat, CD-1 and C57BL/6J mouse) were obtained from BioIVT and the Pfizer Drug and Safety Research & Development (DSRD) tissue bank and pooled by sex. All mouse and rat work was performed according to Pfizer Global Research policies and procedures. Human heart, kidney, liver, and lung were purchased from BioIVT, and human brain was obtained from the NIH NeuroBioBank[54] as a pool of 2 male and 2 female donors. All human tissues were processed following University of Rhode Island and Pfizer Institutional Review Board approved protocols. The equilibrium dialysis device (HTD96) and cellulose membranes with a molecular weight cutoff of 12-14 kDa were obtained from HTDialysis, LLC. All other reagents were purchased from Sigma-Aldrich unless otherwise specified.

2.2 Tissue homogenization and preparation

Tissues were processed according to previously described methods.[47] Briefly, frozen tissues were completely thawed in a 37°C water bath. Small incisions were made to the tissues to minimize blood contamination. Thawed tissues were soaked in Dulbecco's phosphate-buffered saline (DPBS, pH: 7.4, ThermoFisher) for five minutes. The pH in the suspension was measured for all experiments. Tissue samples were subsequently dried with paper towel, weighed, and diluted to either 1:5 or 1:10 (brain) using DPBS. Tissues were homogenized using a TH tissue homogenizer (Omni). In a second step, the tissues were homogenized further using a glass dounce homogenizer (Wheaton).

2.3 Equilibrium Dialysis

The equilibrium dialysis methods used an HTD 96 micro equilibrium device for binding studies that was similar to previously reported techniques.[50-52] Briefly, DBPS buffer solution containing PFAS was prepared. The receiver concentration was ~five-fold the estimated $f_{unbound}$ concentration based on preliminary data using the same test setup or was assumed to be 0.001 (unitless) if no prior data were available. Porous membranes of the dialysis apparatus were pre-saturated twice with 250 µL of PFAS-spiked DBPS buffer for one hour and overnight (~18 h), respectively. Stock solutions of single PFAS in dimethylsulfoxide (DMSO) were prepared and added to tissue homogenates yielding final concentrations of 5 µM (1% DMSO). This concentration was chosen to optimize the LC-MS/MS signal while maintaining a PFAS-to-tissue homogenate ratio that avoids saturation effects observed for proteins like serum albumin.[37,55] 150 µL of PFAS-free DBPS were added to the receiver and 150 µL of PFAS-spiked tissue homogenates were added to the donor side. Replicates *(n*=4) of PFAS:tissue combinations were tested. The HTD was sealed with a gas-permeable membrane (Sigma) and shaken at 200 rpm at 5% CO_2/air, 75% relative humidity, and 37 °C for 18 h. For protein and tissue precipitation, 15 µL of buffer and 45 µL of tissue homogenate were transferred into a 96-deep well plate. To ensure

there were no interferences between wells during the LC-MS/MS run, an additional 45 µL of blank matrix was added to the buffer side and 15 µL of blank buffer to the matrix side in the sample plate to create matrix-matched samples. The samples were quenched with 200 µL of cold acetonitrile containing tolbutamide (30 nM) and carbamazepine (12 nM) that were used as internal standards to monitor the performance of the LC-MS/MS. The plates were sealed, vortexed for 1 min, and centrifuged at 3000 rpm for 5 min. Supernatant was transferred to a new 96-well, evaporated under nitrogen gas, and analyzed by LC-MS/MS. $f_{unbound}$ were calculated as

$$\text{Diluted } f_{\text{unbound,d}} = \frac{\text{Receiver Area Ratio}}{\text{Donor Area Ratio}} \quad (1)$$

$$\text{Undiluted } f_{\text{unbound}} = \frac{1/\text{DF}}{\left(\left(\left({}^{1}/_{f_{\text{unbound,d}}}\right)-1\right)+{}^{1}/_{\text{DF}}\right)} \quad (2)$$

where DF is the dilution factor and $f_{unbound,d}$ is the diluted $f_{unbound}$. All calculations are based on area ratios (analyte/internal standard) within the linear range of calibration curves. Stability and recovery of PFAS concentrations were tested in parallel for all experiments and were above quality control thresholds (>70% recovery) in all experiments for all test compounds. Tissues that were not spiked with PFAS were used as controls and showed no or minimal background levels of the target compounds that did not infer with the data analysis.

2.4 LC-MS/MS Quantification

For analysis, samples were reconstituted in HPLC grade water/acetonitrile 50/50 (v/v) and vortexed for 1 min. LC-MS/MS analyses were performed on a SCIEX Triple Quad 5500 mass spectrometer (SCIEX) equipped with Turbo Ion Spray interface. The full analytical method is described in Section S2 and Table S3 of the Supporting Information (SI).

2.5 Scalar Determination and Statistical Data Analysis

Multiple analyses were conducted to evaluate the relationships between $f_{unbound}$ across tissues and species following previous studies.[47,48] The variability in quadruplicate $f_{unbound}$ were

log normally distributed, justifying the use of a log transformed $f_{unbound}$ for statistical analysis. Geometric mean $f_{unbound}$ values for each PFAS were analyzed across tissues (brain, heart, kidney, liver, lung) and species (human, rat, mouse). To determine if rodent tissues can predict PFAS binding in human tissues, we tested if existing scaling factors that were derived for pharmaceuticals[47] can be used for PFAS. Scaling factors are drug-independent numerical coefficients that account for species-species differences in tissue composition and binding affinity, enabling the extrapolation of drug distribution data from animal models to humans. New scalars for brain tissue $f_{unbound}$ from rat liver for this PFAS set by minimizing sum of squared errors (SSE) between observed and predicted values as

$$\mathrm{SSE} = \sum \left(\ln(\mathrm{Predicted}) - \ln(\mathrm{Observed})\right)^2 \quad (3)$$

Scatterplots on the log scale were used to visualize the strength of relationships between rat liver $f_{unbound}$ and other species/tissue combinations. Mean absolute fold differences (MAFD) and Spearman's rank correlations were used to quantify the agreement and were calculated as the exponentiated mean of absolute log $f_{unbound}$ differences, equivalent to mean absolute error on the log scale. Plots and summary statistics were produced with and without scalars. To evaluate the equivalence of geometric mean $f_{unbound}$ values across species and tissues, we employed the two one-sided tests (TOST) for average bioequivalence.[48,56,57] The TOST procedure tested if the true geometric mean $f_{unbound}$ differences between species/tissue pairs were within a 2-fold difference, resulting in 19 total statistical comparisons. The p-values and confidence intervals were adjusted using the Bonferroni adjustment to maintain a family-wise error rate of 0.05 and corresponding confidence intervals.[58] This test was performed before and after the application of scalars. The TOST procedure was also employed to assess equivalence for similar tissues between species. As all pairwise comparisons of species were assessed, the less conservative ℓ-correction[59] was used to adjust the intervals and maintain a family-wise error rate of 0.05. The data were analyzed using *R*[60] and the plots were created via the ggplot2 package.[61]

2.6 Partial Least Squares Regression (PLSR)

Relationships between PFAS physicochemical properties and $f_{unbound}$ in tissues were investigated using a Partial Least Square Regression (PLSR) multivariate approach. We used $f_{unbound}$ in the liver, brain, heart, kidney, and lung tissue to develop regression models. PLSR is a multivariate approach that allows many responses (i.e., $f_{unbound}$ in various tissues) to be incorporated in one regression model. PLSR performs a descriptor dimension reduction procedure and constructs a set of latent components that maximize the total descriptors variance in the dataset to generate the model with the best predictive power for the target responses. [62] Using the PLSR approach, we developed four models based on the experimental $f_{unbound}$ results obtained from the four organisms: C57, human, mouse, and rat. A total of 20 physicochemical properties were calculated from Molecular Operation Environment (MOE) software version 2018.01 (Chemical Computing Group ULC) and Dragon software version 6.0 (Talete srl). These property descriptors were combined to train and validate the PLSR models for the 16 study PFAS using the standard Leave One Out Cross Validation (LOOCV). In the LOOCV procedure, a PFAS was considered as a test set for model evaluation and the remaining 15 PFAS were used as training set for developing the model. This process was repeated 16 times, such that each PFAS was used as a test set once. Parameters for building the model (i.e., number of components) were tuned using a grid search in the cross-validation process. The optimal number of components was determined to be four for the model developed for humans, and three for the models developed for C57, mouse and rat.

3.0 Results & Discussion

Unbound fractions of PFAS in human and rodent tissues. $f_{unbound}$ in human, rat, and mouse tissues generally decreased with molecular weight (M_w) and octanol-water distribution coefficient (log*D*) of the tested PFAS (Figs. 1, S1, S2). $f_{unbound}$ of the tested PFAS varied by six orders of magnitude (6.8 x 10^{-6} to 0.3), with six of the 16 PFAS being >99.999% bound. The SI contains all data on $f_{unbound}$ and coefficients of variation (Tables S4-S7). Higher molecular weight (M_w) PFAS with longer perfluorinated carbon chains and higher log*D* have high tissue binding affinity, resulting in lower $f_{unbound}$ than the shorter-chain, low M_w PFAS with low log*D*.

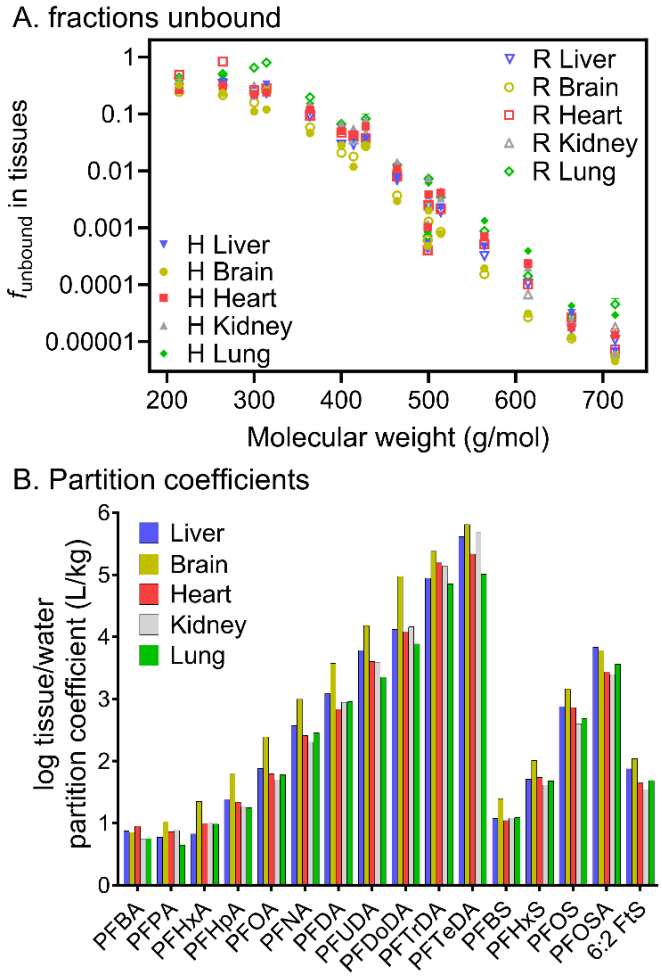

Figure 1. A. $f_{unbound}$ in human ("H") and rat ("R") liver, brain, heart, kidney, and lung tissue plotted against the molecular weight (g/mol) of the 16 study PFAS. B. Tissue/water partition coefficients of the 16 study PFAS in human liver, brain, heart, kidney, and lung tissue.

We observed a strong relationship between M_w and $f_{unbound}$. For example, PFTeDA (M_w: 714) exhibited a low $f_{unbound}$ in human liver tissue (6.8×10^{-6}), in contrast to PFBA (M_w: 214), which showed six orders of magnitude higher $f_{unbound}$ of 0.3. Both PFAS are carboxylic acids, but the increase in fluorinated carbon chain length and lipophilicity resulted in a 45,000x stronger binding of PFTeDA (η_{pfc} = 14; log*D*: 10.11) than PFBA (η_{pfc} = 3; log*D*: 2.2). A similar trend for binding to serum albumin and globulins was recently reported, where carboxylates showed increased binding as M_w increased up until a plateau at a Mw ≈ 500-600 g/mol. [29] Interestingly, this plateau was not observed in this study (Fig. 1). Past work suggested phospholipid concentrations drive accumulation of η_{pfc} ≥10 PFAS in the brains of marine mammals. [63] Accordingly, binding of PFAS to isolated phospholipids increased linearly up until PFDA, [30,64] indicating $f_{unbound}$ of long-chain PFAS to be driven by phospholipid binding more than by protein binding.

Fig. 1B shows the $f_{unbound}$ data converted into $K_{tissue/w}$ values to facilitate comparisons to human tissues. $K_{tissue/w}$ values were highest in brain tissues for 14 of the 16 PFAS. This potentially reflects the high protein and membrane lipid content of human brain tissue, [65] which are known to strongly bind long-chain PFAS. [30,31] Comparable binding among human liver, kidney, and heart tissues was observed, with small variations among the PFAS tested. Binding in lung tissue was relatively low, especially for η_{pfc} = 10-13 carboxylic acids, which may reflect its low phospholipid content. [65]

Strong correlation between PFAS tissue binding in humans and rodents. Pairwise comparisons for all tissues and species demonstrated a strong association between log-transformed $f_{unbound}$ of PFAS between all tissues and species combinations (Figs. 2, S3, R^2 ≥0.97). These results suggest humans and rodents exhibit similar PFAS tissue binding for the brain, heart, lung, liver, and kidney. Spearman Rank Correlations among all the comparisons ranged from 0.96 to 1 (Table S8). These data demonstrate approximate inter-matrix agreement between $f_{unbound}$ of PFAS across the different species and tissue types. A Two One-Sided Tests (TOST)

procedure for multiple comparisons was conducted within tissue pairwise species comparisons $f_{unbound}$ values for all tissues (Fig. S4). A 2-fold difference threshold analysis was employed to determine equivalence.[48,50] Of note, the highest concordance in log-transformed $f_{unbound}$ between human and rodent species was found for human tissues and rat liver (Fig. S5, R^2 ≥0.98), suggesting the utility of rat liver as a model tissue for estimating the binding of PFAS in human tissues.

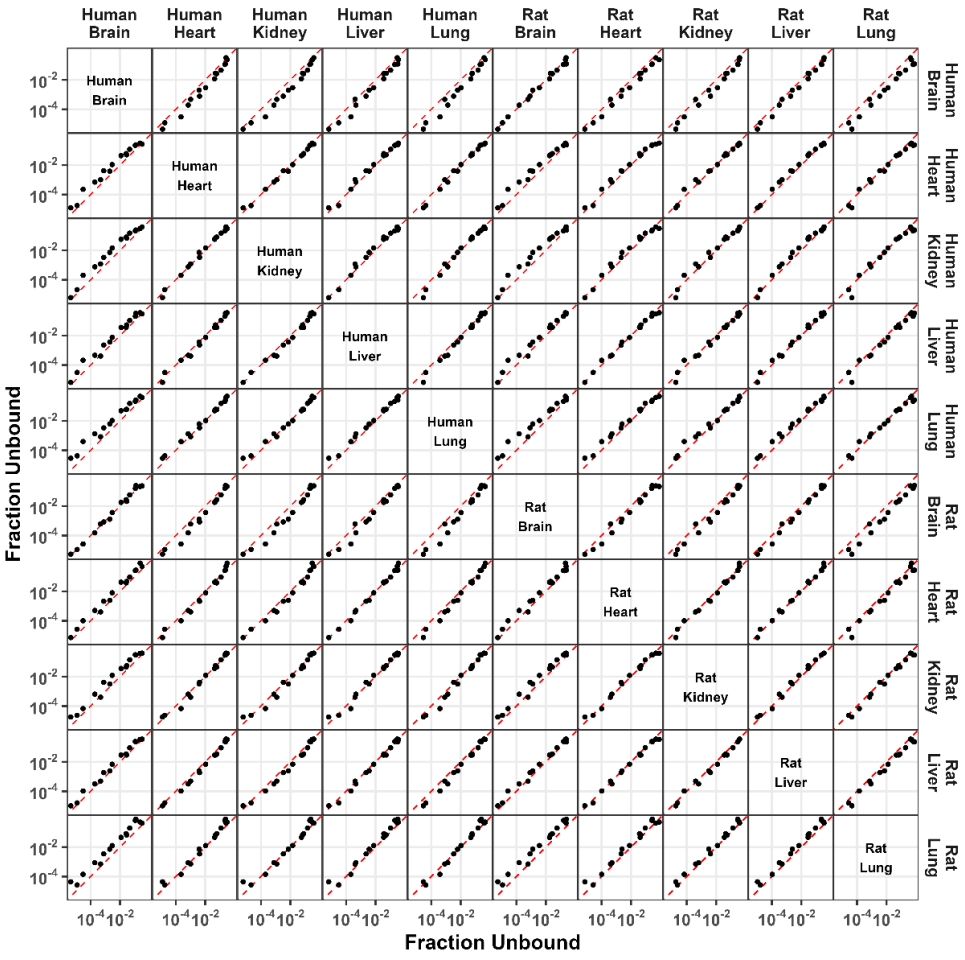

Figure 2. Pairwise comparison of human tissue $f_{unbound}$ versus rat tissue $f_{unbound}$ for brain, heart, kidney, liver, and lung. Red dashed lines indicate 1:1 correlations.

Rat liver as a surrogate for predicting tissue binding of PFAS in humans. Previous work on pharmaceuticals has used rat liver $f_{unbound}$ as a surrogate for estimating $f_{unbound}$ in human heart, liver, lung, kidney, and brain tissues.[47] In this work, $f_{unbound}$ was not found to depend on

species and application of scaling factors for any differences allowed robust predictions of human tissue binding. [66] In this study, we adapted previously established scalars[47] to predict tissue binding of PFAS in humans using rat liver as model tissue. Comparisons of rat liver $f_{unbound}$ against the $f_{unbound}$ for multiple tissues and species, with and without scalars, are shown in Figs 3a and 3b with 2-and 10-fold thresholds. Most comparison matrix pairs had a pre-scalar mean absolute fold difference (MAFD) below 2.0 except for human and rat lung showing an MAFD of 2.04 and 2.21 (Table S9), respectively. The MAFD after applying scalars against rat liver $f_{unbound}$ ranged from 1.19 to 1.57, indicating 2-fold equivalence across all data sets. The Spearman rank correlation of rat liver against all combinations showed a high correlation with a range between 0.965 and 0.997 (Table S9).

Table 1: Equations to scale $f_{unbound}$ from rat liver to human and mouse tissues.

Tissues	Human $f_{unbound}$	Rat (Wistar Han) $f_{unbound}$	Mouse (CD-1; C57BL/6) $f_{unbound}$
Brain	$\frac{1}{\left(1+1.78\cdot\left(\frac{1}{f_{unbound,rat,liver}}-1\right)\right)}$	$\frac{1}{\left(1+1.68\cdot\left(\frac{1}{f_{unbound,rat,liver}}-1\right)\right)}$	$\frac{1}{\left(1+1.64\cdot\left(\frac{1}{f_{unbound,rat,liver}}-1\right)\right)}$ $\frac{1}{\left(1+1.75\cdot\left(\frac{1}{f_{unbound,rat,liver}}-1\right)\right)}$
Heart	$f_{unbound,rat,liver}$	$f_{unbound,rat,liver}$	$f_{unbound,rat,liver}$
Kidney	$\frac{1}{\left(1+0.462\cdot\left(\frac{1}{f_{unbound,rat,liver}}-1\right)\right)}$	$\frac{1}{\left(1+0.589\cdot\left(\frac{1}{f_{unbound,rat,liver}}-1\right)\right)}$	$\frac{1}{\left(1+0.761\cdot\left(\frac{1}{f_{unbound,rat,liver}}-1\right)\right)}$
Liver	$f_{unbound,rat,liver}$	$f_{unbound,rat,liver}$	$f_{unbound,rat,liver}$
Lung	$\frac{1}{\left(1+0.468\cdot\left(\frac{1}{f_{unbound,rat,liver}}-1\right)\right)}$	$\frac{1}{\left(1+0.359\cdot\left(\frac{1}{f_{unbound,rat,liver}}-1\right)\right)}$	$\frac{1}{\left(1+0.416\cdot\left(\frac{1}{f_{unbound,rat,liver}}-1\right)\right)}$

Bonferroni adjusted TOST analysis across all species and tissues against rat liver $f_{unbound}$ values before and after applying scaling factors improved concordance between species (Fig. 3).

New scaling factors for brain tissue were estimated based on our PFAS data set (Table 1). The agreement between rodent and human $f_{unbound}$, when applying scalars previously derived for pharmaceuticals, [47] validates their use for extrapolating PFAS tissue binding across species. Using the scalars, all tissue types were statistically 2-fold equivalent to rat liver, except brain (Fig. 3). Rat brain was concordant with rat liver for pharmaceuticals, [47] this was not the case for our PFAS data set. The higher binding for brain in this study may be due to the higher phospholipid content of brain compared to other tissues. [67] For example, PFOSA (log*D*: 5.5) had a MAFD of 1.02 when comparing liver against brain for all species, whereas PFOS (log*D*: 6.8) had a MAFD of 2.06. Although brain binding for all species was not within the 2-fold equivalency threshold, data were within 3-fold. Overall, our study suggests equivalence of $f_{unbound}$ values between all groups against rat liver when scaling factors[47] are applied, suggesting rat liver can be used as a surrogate for predicting PFAS tissue binding in future studies.

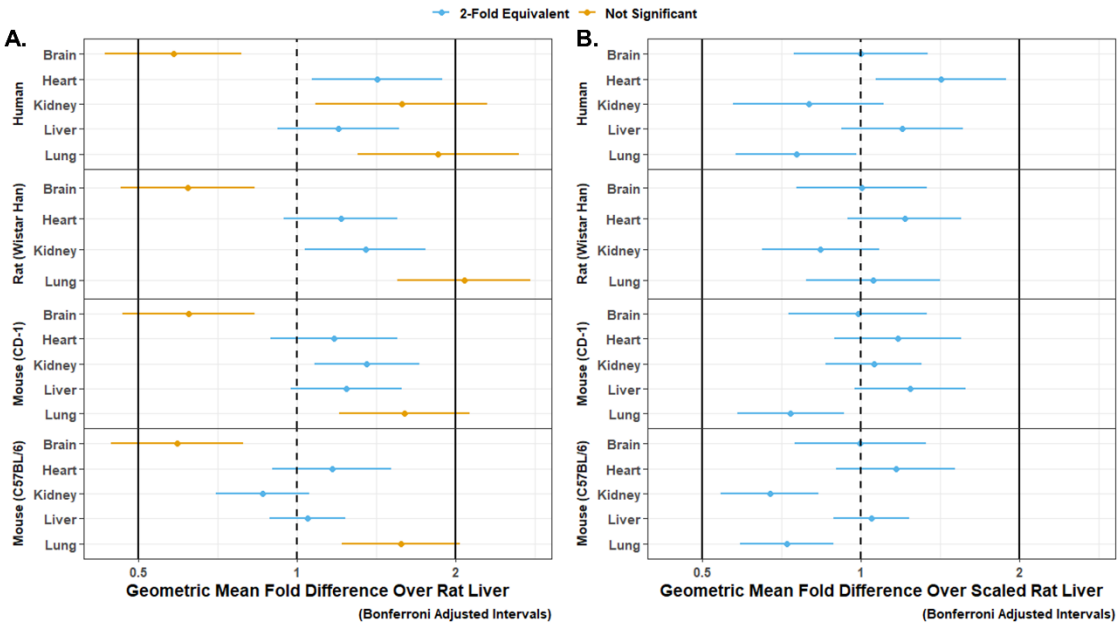

Figure 3. Bonferroni adjusted Two One-Sided Tests (TOST) procedure analysis tissue $f_{unbound}$ equivalence test against rat liver $f_{unbound}$ with unscaled (A) and scaled (B) values.

Physicochemical properties drive tissue binding of PFAS. Results of this study show

a clear relationship between PFAS molecular weight and $f_{unbound}$, as well as log*D* and $f_{unbound}$ (Figs. 1, S1). As a next step, we applied Partial Least Squares Regression modeling to investigate the relationship between 20 physicochemical properties of PFAS and their $f_{unbound}$ in tissues of the four species/strains (human, rat, CD-1 mouse, and C57BL/6 mouse). The results demonstrated strong associations between physicochemical properties and $f_{unbound}$ (Table S10). The correlation coefficients (R^2) of leave one out cross validation are in the range from 0.95 to 0.99. By conducting a descriptor analysis on the resulting models, we assessed the relative importance of individual physicochemical properties of PFAS to their overall tissue binding, based on their mean coefficients in determining log-transformed $f_{unbound}$ (Table S11). Molecular weight and p*K*a were found to have the highest contributions to predict $f_{unbound}$ among all 20 physicochemical descriptors in resulted models (Table S11). All three lipophilicity descriptors, especially log*D*, contributed positively to $f_{unbound}$ predictions (mean coefficients > 0). These results agree with previous studies that demonstrated significant correlations between molecular weight, hydrophobicity, fluorinated carbon chain length and the binding strength of PFAS to isolated tissue macromolecules like albumin[29,38,41,42], structural proteins, [31] and phospholipids. [30,44]

Significance of tissue binding to PFAS toxicokinetics. The generally strong and M_w-dependent $f_{unbound}$ of PFAS in tissues suggest that tissue binding is essential for understanding the distribution and the accumulation within tissues. Results showed binding of PFAS was comparable between liver, kidney, and heart tissues. This suggests that specific binding proteins may be less critical for tissue accumulation than previously postulated. For example, the liver is enriched in liver-type fatty acid binding proteins (L-FABP), yet tissue binding to liver was comparable to other tissues (≤2-fold difference for 14/16 PFAS). This indicates that L-FABP may be less important for tissue retention than previously suggested. [68] Data from this study suggest that macromolecules (e.g., structural proteins, phospholipids) that have comparable contents among tissues are the primary drivers of relatively small differences in $f_{unbound}$.

Comparability to animal studies and human cohorts. The long half-lives of long-chain PFAS in humans are thought to be a function of strong tissue binding.[69] Differences between human and rodent toxicokinetics have been proposed as factors affecting PFAS exposures. For example, organic anion transporters (OATs),[70] organic anion transporting polypeptides (OATPs),[71] and permeability have all been proposed as important determinants of human exposures.[44] However, PFAS bound in tissues are unavailable for elimination from the circulatory system through renal and biliary clearance.[35] Notably, we found that $f_{unbound}$ correlates well with elimination half-lives of PFAS in humans (Fig. S6). For example, the $f_{unbound}$ of PFOS in human tissues was 5.8-11.3 times lower than for PFOA, which corresponds to the difference in observed elimination half-lives between the two PFAS (PFOA: 3.8 years, PFOS: 5.4 years).[23]

Previous rat and mouse studies reported liver PFOS concentrations that were ~20-fold higher than in lung and kidney tissue.[22,72] In contrast, our results suggest liver/kidney and liver/lung concentration ratios of 0.53 and 1.5. Rodent studies using oral administration may not reflect steady-state exposures in humans because PFAS pass the gastrointestinal barrier and may accumulate in the liver after absorption from the gut. In this work, tissue/tissue concentration ratios derived from experimental $K_{tissue/w}$ were compared to equivalent concentration ratios measured in human cohort studies. Interestingly, liver/tissue concentration ratios were similar between binding experiments and in humans for the long-chain PFNA and PFOS (η_{pfc} = 8), whereas PFHxS (η_{pfc} = 6) and PFOA (η_{pfc} = 7) were overestimated in the liver as compared to kidney and lung tissue (Fig. S7). These comparisons indicate that for long-chain PFAS, tissue binding is the major driver for elimination and tissue distribution in humans. Exposure to short-chain PFAS may be driven by complex kinetic processes like membrane transporters,[73,74] permeability,[44] renal reabsorption,[75] and hepatic recirculation.[76]

Although the brain shows the highest sorption capacity for PFAS in our experiments, low concentrations of PFAS have been measured in human brains relative to liver, kidney, and lung

346 tissues (Fig. S7). [19,21] The lower relative tissue distribution of PFOS and PFOA to brain was also
347 observed in rats. [22,72] The limited distribution to brain *in vivo* is likely the result of the protective
348 effects of the blood-brain barrier[77-79] because strong acids are typically restricted from crossing.
349 [80] Future studies are needed to assess to what extent tissue binding experiments reflect PFAS
350 exposures observed in other human tissues (e.g., spleen, mammary gland).

351 **Implications for characterizing toxicokinetics of PFAS in humans.** In this study, we
352 conducted binding experiments using five tissues from common animal model species (i.e.,
353 mouse and rat) and humans for 16 study PFAS to: (i) evaluate species and tissue-specific binding
354 and (ii) elucidate mechanistic understanding of factors affecting accumulation and elimination.
355 Results show only small differences in tissue binding across biological species. We find rat liver
356 provides a suitable surrogate tissue for predicting binding of PFAS in various human tissues
357 (kidney, brain, lung, heart) when used in combination with appropriate scaling factors.
358 Considering the large number and structural heterogeneity of PFAS, rat liver provides a useful
359 surrogate for screening and categorizing the internal distribution of PFAS in humans. To reduce
360 animal use, future studies should explore alternative surrogate materials, such as polymers
361 known to bind PFAS, to predict human tissue binding of these compounds. Data on $f_{unbound}$ and
362 $K_{tissue/w}$ reported in this study can help parameterize physiologically-based toxicokinetic (PBTK)
363 models that are useful for quantifying the elimination and distribution of PFAS. However, it is
364 important to consider that other toxicokinetic processes, which may be more species-dependent
365 than tissue binding, such as membrane transporter expression, could introduce inaccuracies
366 when applying the predicted $f_{unbound}$ in human PBTK models. Still, human and modeling studies
367 both suggest tissue binding is a major factor driving PFAS exposure and elimination. [19,20] Future
368 studies should assess the variability in tissue $f_{unbound}$ among humans that result from genetic or
369 disease-related differences in tissue protein and lipid composition, such as lipid accumulation in
370 fatty liver disease. [81] The predictive framework presented in this study may be useful for assessing
371 potential accumulation of emerging PFAS with more complex structural and physicochemical

properties, which are increasingly detected in the environment. Understanding their distribution among human tissues will help inform regulations to control their production and release into the environment, reducing their uptake through drinking water and food.

Supporting Information

Information on PFAS chemicals tested in this study; LC-MS/MS quantification method; Unbound fraction data; Pairwise comparisons of $f_{unbound}$; Statistical analyses; PLSR model results; Unbound fractions compared to elimination half-lives and tissue distributions in humans.

Acknowledgements

This study was partially supported by the National Institute of Environmental Health Sciences (Grants R01ES031080, R35ES031709, and P42ES027706), National Institute of General Medical Sciences (Grant R01GM148743), National Institute of Child Health and Human Development (Grant UHD113039), and National Science Foundation (Grant 2402311). The authors would like to thank the NIH Neurobiobank for the fulfilment of Human Brain Tissue used in this study. The authors would like to thank Roberta King, Rainer Lohmann, Emily Kaye, Andrew Kim, Olga Skende, Andrew Kim, and Danielle Warila at The University of Rhode Island and colleagues at Pfizer (Li Di, Varma Manthena) for discussion and feedback. The TOC art was created by the authors with BioRender.com.

References

1. Wang, Z.; DeWitt, J. C.; Higgins, C. P.; Cousins, I. T., A Never-Ending Story of Per- and Polyfluoroalkyl Substances (PFASs)? *Environ Sci Technol* **2017,** *51*, (5), 2508-2518.
2. Giesy, J. P.; Kannan, K., Global distribution of perfluorooctane sulfonate in wildlife. *Environ Sci Technol* **2001,** *35*, (7), 1339-42.
3. Martinez, B.; Da Silva, B. F.; Aristizabal-Henao, J. J.; Denslow, N. D.; Osborne, T. Z.; Morrison, E. S.; Bianchi, T. S.; Bowden, J. A., Increased levels of perfluorooctanesulfonic acid (PFOS) during Hurricane Dorian on the east coast of Florida. *Environ Res* **2022,** *208*, 112635.

4. Thompson, J.; Roach, A.; Eaglesham, G.; Bartkow, M. E.; Edge, K.; Mueller, J. F., Perfluorinated alkyl acids in water, sediment and wildlife from Sydney Harbour and surroundings. *Mar Pollut Bull* **2011,** *62*, (12), 2869-75.
5. Yu, X.; Dunstan, J.; Jacobson, S. W.; Molteno, C. D.; Lindinger, N. M.; Turesky, T. K.; Meintjes, E. M.; Jacobson, J. L.; Gaab, N., Distinctive neural correlates of phonological and reading impairment in fetal alcohol-exposed adolescents with and without facial dysmorphology. *Neuropsychologia* **2022,** *169*, 108188.
6. Nystrom, J.; Benskin, J. P.; Plassmann, M.; Sandblom, O.; Glynn, A.; Lampa, E.; Gyllenhammar, I.; Moraeus, L.; Lignell, S., Demographic, life-style and physiological determinants of serum per- and polyfluoroalkyl substance (PFAS) concentrations in a national cross-sectional survey of Swedish adolescents. *Environ Res* **2022,** *208*, 112674.
7. Hu, X. D. C.; Andrews, D. Q.; Lindstrom, A. B.; Bruton, T. A.; Schaider, L. A.; Grandjean, P.; Lohmann, R.; Carignan, C. C.; Blum, A.; Balan, S. A.; Higgins, C. P.; Sunderland, E. M., Detection of Poly- and Perfluoroalkyl Substances (PFASs) in US Drinking Water Linked to Industrial Sites, Military Fire Training Areas, and Wastewater Treatment Plants. *Environ Sci Tech Let* **2016,** *3*, (10), 344-350.
8. Barber, J. L.; Berger, U.; Chaemfa, C.; Huber, S.; Jahnke, A.; Temme, C.; Jones, K. C., Analysis of per- and polyfluorinated alkyl substances in air samples from Northwest Europe. *J Environ Monitor* **2007,** *9*, (6), 530-541.
9. Holder, C.; DeLuca, N.; Luh, J.; Alexander, P.; Minucci, J. M.; Vallero, D. A.; Thomas, K.; Hubal, E. A. C., Systematic Evidence Mapping of Potential Exposure Pathways for Per- and Polyfluoroalkyl Substances Based on Measured Occurrence in Multiple Media. *Environmental Science & Technology* **2023,** *57*, (13), 5107-5116.
10. Centers for Disease Control and Prevention (CDC). National Center for Health Statistics (NCHS). National Health and Nutrition Examination Survey Data. Hyattsville, MD: U.S. Department of Health and Human Services, Centers for Disease Control and Prevention, [2024] [https://wwwn.cdc.gov/nchs/nhanes/].
11. Olsen, G. W.; Mair, D. C.; Lange, C. C.; Harrington, L. M.; Church, T. R.; Goldberg, C. L.; Herron, R. M.; Hanna, H.; Nobiletti, J. B.; Rios, J. A.; Reagen, W. K.; Ley, C. A., Per- and polyfluoroalkyl substances (PFAS) in American Red Cross adult blood donors, 2000-2015. *Environmental Research* **2017,** *157*, 87-95.
12. Kato, K.; Wong, L. Y.; Jia, L. T.; Kuklenyik, Z.; Calafat, A. M., Trends in Exposure to Polyfluoroalkyl Chemicals in the US Population: 1999-2008. *Environmental Science & Technology* **2011,** *45*, (19), 8037-8045.
13. Calafat, A. M.; Wong, L. Y.; Kuklenyik, Z.; Reidy, J. A.; Needham, L. L., Polyfluoroalkyl chemicals in the US population: Data from the National Health and Nutrition Examination Survey (NHANES) 2003-2004 and comparisons with NHANES 1999-2000. *Environ Health Persp* **2007,** *115*, (11), 1596-1602.
14. Grandjean, P.; Heilmann, C.; Weihe, P.; Nielsen, F.; Mogensen, U. B.; Timmermann, A.; Budtz-Jørgensen, E., Estimated exposures to perfluorinated compounds in infancy predict attenuated vaccine antibody concentrations at age 5-years. *J Immunotoxicol* **2017,** *14*, (1), 188-195.
15. Averina, M.; Brox, J.; Huber, S.; Furberg, A. S., Exposure to perfluoroalkyl substances (PFAS) and dyslipidemia, hypertension and obesity in adolescents. The Fit Futures study. *Environ Res* **2021,** *195*, 110740.
16. Ducatman, A.; Fenton, S. E., Invited Perspective: PFAS and Liver Disease: Bringing All the Evidence Together. *Environmental Health Perspectives* **2022,** *130*, (4), 041303.
17. Fenton, S. E.; Ducatman, A.; Boobis, A.; DeWitt, J. C.; Lau, C.; Ng, C.; Smith, J. S.; Roberts, S. M., Per- and Polyfluoroalkyl Substance Toxicity and Human Health Review: Current State of Knowledge and Strategies for Informing Future Research. *Environ Toxicol Chem* **2021,** *40*, (3), 606-630.
18. Boston, C. M.; Banacos, N.; Heiger-Bernays, W., Per- and Polyfluoroalkyl Substances: A National Priority for Safe Drinking Water. *Public Health Rep* **2019,** *134*, (2), 112-117.

19. Nielsen, F.; Fischer, F. C.; Leth, P. M.; Grandjean, P., Occurrence of Major Perfluorinated Alkylate Substances in Human Blood and Target Organs. *Environmental Science & Technology* **2024,** *58*, (1), 143-149.
20. Baumert, B. O.; Fischer, F. C.; Nielsen, F.; Grandjean, P.; Bartell, S.; Stratakis, N.; Walker, D. I.; Valvi, D.; Kohli, R.; Inge, T.; Ryder, J.; Jenkins, T.; Sisley, S.; Xanthakos, S.; Rock, S.; La Merrill, M. A.; Conti, D.; McConnell, R.; Chatzi, L., Paired Liver:Plasma PFAS Concentration Ratios from Adolescents in the Teen-LABS Study and Derivation of Empirical and Mass Balance Models to Predict and Explain Liver PFAS Accumulation. *Environmental Science & Technology* **2023**, 57, 40, 14817–14826.
21. Pérez, F.; Nadal, M.; Navarro-Ortega, A.; Fàbrega, F.; Domingo, J. L.; Barceló, D.; Farré, M., Accumulation of perfluoroalkyl substances in human tissues. *Environ Int* **2013,** *59*, 354-62.
22. Chang, S. C.; Noker, P. E.; Gorman, G. S.; Gibson, S. J.; Hart, J. A.; Ehresman, D. J.; Butenhoff, J. L., Comparative pharmacokinetics of perfluorooctanesulfonate (PFOS) in rats, mice, and monkeys. *Reprod Toxicol* **2012,** *33*, (4), 428-440.
23. Olsen, G. W.; Burris, J. M.; Ehresman, D. J.; Froehlich, J. W.; Seacat, A. M.; Butenhoff, J. L.; Zobel, L. R., Half-life of serum elimination of perfluorooctanesulfonate,perfluorohexanesulfonate, and perfluorooctanoate in retired fluorochemical production workers. *Environ Health Perspect* **2007,** *115*, (9), 1298-305.
24. Zhang, Y.; Beesoon, S.; Zhu, L.; Martin, J. W., Biomonitoring of perfluoroalkyl acids in human urine and estimates of biological half-life. *Environ Sci Technol* **2013,** *47*, (18), 10619-27.
25. Olsen, G. W.; Chang, S. C.; Noker, P. E.; Gorman, G. S.; Ehresman, D. J.; Lieder, P. H.; Butenhoff, J. L., A comparison of the pharmacokinetics of perfluorobutanesulfonate (PFBS) in rats, monkeys, and humans. *Toxicology* **2009,** *256*, (1-2), 65-74.
26. Jian, J. M.; Chen, D.; Han, F. J.; Guo, Y.; Zeng, L. X.; Lu, X. W.; Wang, F., A short review on human exposure to and tissue distribution of per- and polyfluoroalkyl substances (PFASs). *Science of the Total Environment* **2018,** *636*, 1058-1069.
27. Kim, S. J.; Heo, S. H.; Lee, D. S.; Hwang, I. G.; Lee, Y. B.; Cho, H. Y., Gender differences in pharmacokinetics and tissue distribution of 3 perfluoroalkyl and polyfluoroalkyl substances in rats. *Food Chem Toxicol* **2016,** *97*, 243-255.
28. Marques, E. S.; Agudelo, J.; Kaye, E. M.; Modaresi, S. M. S.; Pfohl, M.; Becanova, J.; Wei, W.; Polunas, M.; Goedken, M.; Slitt, A. L., The role of maternal high fat diet on mouse pup metabolic endpoints following perinatal PFAS and PFAS mixture exposure. *Toxicology* **2021,** *462*, 152921.
29. Fischer, F. C.; Ludtke, S.; Thackray, C.; Pickard, H. M.; Haque, F.; Dassuncao, C.; Endo, S.; Schaider, L.; Sunderland, E. M., Binding of Per- and Polyfluoroalkyl Substances (PFAS) to Serum Proteins: Implications for Toxicokinetics in Humans. *Environmental Science & Technology* **2024,** *58*, (2), 1055-1063.
30. Droge, S. T. J., Membrane-Water Partition Coefficients to Aid Risk Assessment of Perfluoroalkyl Anions and Alkyl Sulfates. *Environmental Science & Technology* **2019,** *53*, (2), 760-770.
31. Allendorf, F.; Goss, K.-U.; Ulrich, N., Estimating the Equilibrium Distribution of Perfluoroalkyl Acids and 4 of Their Alternatives in Mammals. *Environ Toxicol Chem* **2021,** *40*, (3), 910-920.
32. Sunderland, E. M.; Hu, X. D. C.; Dassuncao, C.; Tokranov, A. K.; Wagner, C. C.; Allen, J. G., A review of the pathways of human exposure to poly- and perfluoroalkyl substances (PFASs) and present understanding of health effects. *J Expo Sci Env Epid* **2019,** *29*, (2), 131-147.
33. Di, L.; Breen, C.; Chambers, R.; Eckley, S. T.; Fricke, R.; Ghosh, A.; Harradine, P.; Kalvass, J. C.; Ho, S.; Lee, C. A.; Marathe, P.; Perkins, E. J.; Qian, M.; Tse, S.; Yan, Z. Y.; Zamek-Gliszczynski, M. J., Industry Perspective on Contemporary Protein-Binding Methodologies: Considerations for Regulatory Drug-Drug Interaction and Related Guidelines on Highly Bound Drugs. *J Pharm Sci-Us* **2017,** *106*, (12), 3442-3452.

34. Margolis, J. M.; Obach, R. S., Impact of nonspecific binding to microsomes and phospholipid on the inhibition of cytochrome P4502D6: Implications for relating in vitro inhibition data to in vivo drug interactions. *Drug Metabolism and Disposition* **2003,** *31*, (5), 606-611.
35. Summerfield, S. G.; Yates, J. W. T.; Fairman, D. A., Free Drug Theory - No Longer Just a Hypothesis? *Pharm Res* **2022,** *39*, (2), 213-222.
36. Smeltz, M.; Wambaugh, J. F.; Wetmore, B. A., Plasma Protein Binding Evaluations of Per- and Polyfluoroalkyl Substances for Category-Based Toxicokinetic Assessment. *Chemical Research in Toxicology* **2023,** *36*, (6), 870-881.
37. Qin, W.; Henneberger, L.; Huchthausen, J.; König, M.; Escher, B. I., Role of bioavailability and protein binding of four anionic perfluoroalkyl substances in cell-based bioassays for quantitative in vitro to in vivo extrapolations. *Environ Int* **2023,** *173*, 107857.
38. Alesio, J. L.; Slitt, A.; Bothun, G. D., Critical new insights into the binding of poly- and perfluoroalkyl substances (PFAS) to albumin protein. *Chemosphere* **2022,** *287*, 131979.
39. Smith, D. A.; Di, L.; Kerns, E. H., The effect of plasma protein binding on in vivo efficacy: misconceptions in drug discovery. *Nat Rev Drug Discov* **2010,** *9*, (12), 929-39.
40. Bischel, H. N.; MacManus-Spencer, L. A.; Zhang, C.; Luthy, R. G., Strong associations of short-chain perfluoroalkyl acids with serum albumin and investigation of binding mechanisms. *Environ Toxicol Chem* **2011,** *30*, (11), 2423-2430.
41. Allendorf, F.; Berger, U.; Goss, K. U.; Ulrich, N., Partition coefficients of four perfluoroalkyl acid alternatives between bovine serum albumin (BSA) and water in comparison to ten classical perfluoroalkyl acids. *Environ Sci-Proc Imp* **2019,** *21*, (11), 1852-1863.
42. Crisalli, A. M.; Cai, A.; Cho, B. P., Probing the Interactions of Perfluorocarboxylic Acids of Various Chain Lengths with Human Serum Albumin: Calorimetric and Spectroscopic Investigations. *Chemical Research in Toxicology* **2023,** *36*, (4), 703-713.
43. Zhang, L.; Ren, X.-M.; Guo, L.-H., Structure-Based Investigation on the Interaction of Perfluorinated Compounds with Human Liver Fatty Acid Binding Protein. *Environmental Science & Technology* **2013,** *47*, (19), 11293-11301.
44. Ebert, A.; Allendorf, F.; Berger, U.; Goss, K. U.; Ulrich, N., Membrane/Water Partitioning and Permeabilities of Perfluoroalkyl Acids and Four of their Alternatives and the Effects on Toxicokinetic Behavior. *Environmental Science & Technology* **2020,** *54*, (8), 5051-5061.
45. Cao, H.; Peng, J.; Zhou, Z.; Yang, Z.; Wang, L.; Sun, Y.; Wang, Y.; Liang, Y., Investigation of the Binding Fraction of PFAS in Human Plasma and Underlying Mechanisms Based on Machine Learning and Molecular Dynamics Simulation. *Environmental Science & Technology* **2022**, 57, 46, 17762–17773.
46. Di, L.; Umland, J. P.; Chang, G.; Huang, Y.; Lin, Z.; Scott, D. O.; Troutman, M. D.; Liston, T. E., Species independence in brain tissue binding using brain homogenates. *Drug Metab Dispos* **2011,** *39*, (7), 1270-7.
47. Ryu, S.; Tess, D.; Chang, G.; Keefer, C.; Burchett, W.; Steeno, G. S.; Novak, J. J.; Patel, R.; Atkinson, K.; Riccardi, K.; Di, L., Evaluation of Fraction Unbound Across 7 Tissues of 5 Species. *J Pharm Sci* **2020,** *109*, (2), 1178-1190.
48. Riccardi, K.; Ryu, S.; Lin, J.; Yates, P.; Tess, D.; Li, R.; Singh, D.; Holder, B. R.; Kapinos, B.; Chang, G.; Di, L., Comparison of Species and Cell-Type Differences in Fraction Unbound of Liver Tissues, Hepatocytes, and Cell Lines. *Drug Metab Dispos* **2018,** *46*, (4), 415-421.
49. Read, K. D.; Braggio, S., Assessing brain free fraction in early drug discovery. *Expert Opin Drug Metab Toxicol* **2010,** *6*, (3), 337-44.
50. Riccardi, K.; Cawley, S.; Yates, P. D.; Chang, C.; Funk, C.; Niosi, M.; Lin, J.; Di, L., Plasma Protein Binding of Challenging Compounds. *J Pharm Sci* **2015,** *104*, (8), 2627-36.
51. Ryu, S.; Tess, D.; Di, L., Addressing the Accuracy of Plasma Protein Binding Measurement for Highly Bound Compounds Using the Dilution Method. *AAPS J* **2022,** *25*, (1), 7.

52. Ryu, S.; Riccardi, K.; Patel, R.; Zueva, L.; Burchett, W.; Di, L., Applying Two Orthogonal Methods to Assess Accuracy of Plasma Protein Binding Measurements for Highly Bound Compounds. *J Pharm Sci* **2019,** *108*, (11), 3745-3749.
53. The Interstate Technology & Regulatory Council PFAS, T., Per- and Polyfluoroalkyl Substances Technical and Regulatory Guidance. 2022.
54. Freund, M.; Taylor, A.; Ng, C.; Little, A. R., Chapter 4 - The NIH NeuroBioBank: creating opportunities for human brain research. In *Handbook of Clinical Neurology*, Huitinga, I.; Webster, M. J., Eds. Elsevier: 2018; Vol. 150, pp 41-48.
55. Li, W.; Hu, Y.; Bischel, H. N., In-Vitro and In-Silico Assessment of Per- and Polyfluoroalkyl Substances (PFAS) in Aqueous Film-Forming Foam (AFFF) Binding to Human Serum Albumin. *Toxics* **2021,** *9*, (3), 63.
56. Schuirmann, D. J., A comparison of the two one-sided tests procedure and the power approach for assessing the equivalence of average bioavailability. *J Pharmacokinet Biopharm* **1987,** *15*, (6), 657-80.
57. Walker, E.; Nowacki, A. S., Understanding equivalence and noninferiority testing. *J Gen Intern Med* **2011,** *26*, (2), 192-6.
58. Serlin, R. C., Confidence-Intervals and the Scientific Method - a Case for Holm on the Range. *J Exp Educ* **1993,** *61*, (4), 350-360.
59. Lauzon, C.; Caffo, B., Easy Multiplicity Control in Equivalence Testing Using Two One-Sided Tests. *Am Stat* **2009,** *63*, (2), 147-154.
60. Team, R. C. R: A language and environment for statistical computing. R Foundation for Statistical Computing,. https://www.R-project.org/ (accessed 2024-04-11)
61. Wickham, H., ggplot2 Elegant Graphics for Data Analysis Introduction. *Use R* **2009**, 1-+.
62. Abdi, H., Partial least squares regression and projection on latent structure regression (PLS Regression). *Wires Comput Stat* **2010,** *2*, (1), 97-106.
63. Dassuncao, C.; Pickard, H.; Pfohl, M.; Tokranov, A. K.; Li, M. L.; Mikkelsen, B.; Slitt, A.; Sunderland, E. M., Phospholipid Levels Predict the Tissue Distribution of Poly- and Perfluoroalkyl Substances in a Marine Mammal. *Environ Sci Tech Let* **2019,** *6*, (3), 119-125.
64. Ebert, A.; Allendorf, F.; Berger, U.; Goss, K. U.; Ulrich, N., Membrane/Water Partitioning and Permeabilities of Perfluoroalkyl Acids and Four of their Alternatives and the Effects on Toxicokinetic Behavior. *Environ Sci Technol* **2020,** *54*, (8), 5051-5061.
65. Ruark, C. D.; Hack, C. E.; Robinson, P. J.; Mahle, D. A.; Gearhart, J. M., Predicting Passive and Active Tissue:Plasma Partition Coefficients: Interindividual and Interspecies Variability. *J Pharm Sci-Us* **2014,** *103*, (7), 2189-2198.
66. Hsu, F.; Chen, Y. C.; Broccatelli, F., Evaluation of Tissue Binding in Three Tissues across Five Species and Prediction of Volume of Distribution from Plasma Protein and Tissue Binding with an Existing Model. *Drug Metabolism and Disposition* **2021,** *49*, (4), 330-336.
67. Yoon, J. H.; Seo, Y.; Jo, Y. S.; Lee, S.; Cho, E.; Cazenave-Gassiot, A.; Shin, Y. S.; Moon, M. H.; An, H. J.; Wenk, M. R.; Suh, P. G., Brain lipidomics: From functional landscape to clinical significance. *Sci Adv* **2022,** *8*, (37).
68. Jia, Y.; Zhu, Y.; Xu, D.; Feng, X.; Yu, X.; Shan, G.; Zhu, L., Insights into the Competitive Mechanisms of Per- and Polyfluoroalkyl Substances Partition in Liver and Blood. *Environmental Science & Technology* **2022,** *56*, (10), 6192-6200.
69. Gibaldi, M.; Levy, G.; McNamara, P. J., Effect of plasma protein and tissue binding on the biologic half-life of drugs. *Clin Pharmacol Ther* **1978,** *24*, (1), 1-4.
70. Weaver, Y. M.; Ehresman, D. J.; Butenhoff, J. L.; Hagenbuch, B., Roles of rat renal organic anion transporters in transporting perfluorinated carboxylates with different chain lengths. *Toxicol Sci* **2010,** *113*, (2), 305-14.

71. Zhao, W.; Zitzow, J. D.; Weaver, Y.; Ehresman, D. J.; Chang, S. C.; Butenhoff, J. L.; Hagenbuch, B., Organic Anion Transporting Polypeptides Contribute to the Disposition of Perfluoroalkyl Acids in Humans and Rats. *Toxicological Sciences* **2017,** *156*, (1), 84-95.
72. Bogdanska, J.; Borg, D.; Bergstrom, U.; Mellring, M.; Bergman, A.; DePierre, J.; Nobel, S., Tissue distribution of C-14-labelled perfluorooctanoic acid in adult mice after 1-5 days of dietary exposure to an experimental dose or a lower dose that resulted in blood levels similar to those detected in exposed humans. *Chemosphere* **2020,** *239*.
73. Yang, C.-H.; Glover, K. P.; Han, X., Organic anion transporting polypeptide (Oatp) 1a1-mediated perfluorooctanoate transport and evidence for a renal reabsorption mechanism of Oatp1a1 in renal elimination of perfluorocarboxylates in rats. *Toxicol Lett* **2009,** *190*, (2), 163-171.
74. Yang, C.-H.; Glover, K. P.; Han, X., Characterization of Cellular Uptake of Perfluorooctanoate via Organic Anion-Transporting Polypeptide 1A2, Organic Anion Transporter 4, and Urate Transporter 1 for Their Potential Roles in Mediating Human Renal Reabsorption of Perfluorocarboxylates. *Toxicol Sci* **2010,** *117*, (2), 294-302.
75. Worley, R. R.; Fisher, J., Application of physiologically-based pharmacokinetic modeling to explore the role of kidney transporters in renal reabsorption of perfluorooctanoic acid in the rat. *Toxicol Appl Pharm* **2015,** *289*, (3), 428-441.
76. Cao, H.; Zhou, Z.; Hu, Z.; Wei, C.; Li, J.; Wang, L.; Liu, G.; Zhang, J.; Wang, Y.; Wang, T.; Liang, Y., Effect of Enterohepatic Circulation on the Accumulation of Per- and Polyfluoroalkyl Substances: Evidence from Experimental and Computational Studies. *Environmental Science & Technology* **2022,** *56*, (5), 3214-3224.
77. Yu, Y. Q.; Wang, C.; Zhang, X. H.; Zhu, J. S.; Wang, L.; Ji, M. H.; Zhang, Z.; Ji, X. M.; Wang, S. L., Perfluorooctane sulfonate disrupts the blood brain barrier through the crosstalk between endothelial cells and astrocytes in mice. *Environmental Pollution* **2020,** *256*.
78. Cui, L.; Zhou, Q. F.; Liao, C. Y.; Fu, J. J.; Jiang, G. B., Studies on the Toxicological Effects of PFOA and PFOS on Rats Using Histological Observation and Chemical Analysis. *Arch Environ Con Tox* **2009,** *56*, (2), 338-349.
79. Liu, L.; Liu, W.; Song, J. L.; Yu, H. Y.; Jin, Y. H.; Oami, K.; Sato, I.; Saito, N.; Tsuda, S., A comparative study on oxidative damage and distributions of perfluorooctane sulfonate (PFOS) in mice at different postnatal developmental stages. *J Toxicol Sci* **2009,** *34*, (3), 245-254.
80. Pardridge, W. M., CNS drug design based on principles of blood-brain barrier transport. *J Neurochem* **1998,** *70*, (5), 1781-1792.
81. Gowda, D.; Shekhar, C.; B. Gowda, S. G.; Chen, Y.; Hui, S.-P., Crosstalk between Lipids and Non-Alcoholic Fatty Liver Disease. *Livers* **2023,** *3*, (4), 687-708.